International Journal of Advanced Research in Electronics and Communication Engineering (IJARECE)
Volume 3, Issue 3, March 2014

Deep Analytical Study of Optical Wireless Communication Systems Performance Efficiency Using Different Modulation Techniques in Turbulence Communication Channels

Ahmed Nabih Zaki Rashed[1*], and Hamdy A. Sharshar[2]
[1,2]Electronics and Electrical Communications Engineering Department
Faculty of Electronic Engineering, Menouf 32951, Menoufia University, EGYPT

Abstract*—This paper has presented the different advanced modulation techniques for free space optical (FSO) communication systems transmission efficiency enhancement and signal quality estimation in weak, medium and strong turbulence communication channels. The bandwidth and power efficiency issues in free space optics (FSO) transmissions are addressed under non return to zero on-off keying (NRZ-OOK), return to zero on-off keying (RZ-OOK), pulse position modulation (N-PPM), pulse amplitude modulation (M-PAM), quadrature amplitude modulation (H-QAM) schemes, and their performance in terms of power and bandwidth efficiencies and the bit error rate (BER) against signal to noise ratio (SNR) are compared analytically. The comparative study of the NRZ-OOK, RZ-OOK, N-PPM, M-PAM, and H-QAM schemes are deeply discussed. As well as the minimum detectable received power is also investigated for different Avalanche photodiode (APD) detector receivers types in different turbulence communication channels.

***Index Terms*— Pulse position modulation, Pulse amplitude modulation, Quadrature amplitude modulation, Power Efficiency, and Bandwidth requirement.**

I. INTRODUCTION

Recently, the need to access wireless local area networks from portable personal computers and mobile devices has grown rapidly. Many of these networks have been designed to support multimedia with high data rates, thus the systems require a large bandwidth. Since radio communication systems have limited available bandwidth, a proposal to use indoor optical wireless communications has received wide interest [1, 2]. The major advantages of optical systems are low cost optical devices and virtually unlimited bandwidth. A non directed link, exploiting the light-reflection characteristics for transmitting data to a receiver, is considered to be the most suitable for optical wireless systems in an indoor environment [2]. This link can be categorized as either line-of-sight (LOS) or diffuse. A diffuse link is preferable because there is no alignment requirement and it is more robust This is an open-access article distributed under the creative commons attribution license, which permits unrestricted use, distribution, and reproduction in any medium, provided the original work is properly cited. to shadowing. However, a diffuse link is more susceptible to corruption by ambient light noise, high signal attenuation, and inter symbol interference caused by multipath dispersion. Thus, a diffuse link needs more transmitted power than an LOS link. A well-approximated indoor free-space optical link with the effects of multipath dispersion was presented in [3]. Nevertheless, the average optical transmitter power level is constrained by concerns about power consumption and eye safety. Furthermore, high capacitance in a large-area photodetector limits the receiver bandwidth. Consequently, a power-efficient and bandwidth-efficient modulation scheme is desirable in an indoor optical wireless channel. Normally, an optical wireless system adopts a simple baseband modulation scheme such as on-off keying (OOK) or pulse-position modulation (PPM).

FSO has now emerged as a commercially viable technology to of data, voice and video within the access networks. RF based wireless networks can offer data rates from tens of Mbps (point-to-multipoint) up to several hundred Mbps (point-to-point) [2]. However, there is a major limitation which these RF systems face and that is due to spectrum congestion. The frequency spectrum is getting congested day by day due to in-creasing bandwidth requirements of present and emerging communication systems. The most efficient solution to this problem is the use of FSO system which guarantees abundant bandwidth. Using an optical carrier, we can get data band-width up to 200 THz where as in RF the usable frequency bandwidth is comparatively lower by a factor of 105. We need not to purchase any spectrum license for FSO link. FSO sys-tem is quick to deploy and redeploy and the cost of FSO sys-tem is lower than RF system [3]. The greatest challenge that FSO faces is the atmospheric turbulence, resulting in signal scattering, absorption and fluctuation[4]. These effects become adverse for a link range exceeding 1 km. Another factor responsible for FSO performance degradation is the atmospheric scintillation. The scintillation effect results in signal fading, due to constructive and destructive interference of the optical beam traversing the atmosphere. For FSO links spanning 500 meters or less, typical scintillation fade margins are 2 to 5 dB, which is less than the margins for atmospheric attenuation, making scintillation in-significant for short range FSO systems. However, in clear air when the atmospheric channel attenuation is less than 1 dB/km and most especially when the link range is in excess of 1 km, scintillation impairs the FSO link availability, attainable error performance and the available link margin significantly. However, in clear atmosphere, with a typical attenuation coefficient of 0.43 dB/km, a longer range FSO (1 km) is easily achievable [5].

The paper is organized in the following sections. Section I has explained the basic principles of different modulation techniques with free space optics transmission which are discussed in more details. Section II has explained the mathematical model equations of different modulation

techniques for free space optics communications enhancement. Section III has presented the simulation results and performance evaluation of different modulation techniques in free space atmospheric turbulence channels and the ways to improve its performance efficiency. Finally, section IV has presented the summary of different useful modulation techniques transmission performance under study in free space optics communications under the same operating conditions.

II. System Model Analysis

The performance of a receiver is often based on the notion of signal to noise ratio (SNR), i.e., the rms signal power over the rms noise power. For photon noise limited performance, the mean SNR for a direct detection system is [3]:

$$SNR = \frac{SNR_0}{\sqrt{\frac{P_{S0}}{P_S} + \sigma_{Si}\, SNR_0}} \quad (1)$$

Where P_{SO} is the signal power in free space, P_S is the mean signal power, σ_{Si} is the scintillation index, and SNR_0 is the free space SNR defined by [4]:

$$SNR_0 = \sqrt{\frac{\eta \lambda P_{S0}}{2hcB}} \quad (2)$$

Where η is the detector quantum efficiency, λ is the laser wavelength, h is Planck's constant, c is the speed of light ($3x10^8$ m/sec), B is the transmission bandwidth. System performances for continuous wave (CW) or single pulse optical systems are based on SNR and fade probability. For digital transmission of information, the performance measure is based on the probability of error, also called the bit error rate BER. The scintillation index σ_{Si} can be expressed in term of α and β as follows:

$$\sigma_{Si} = \frac{1}{\alpha} + \frac{1}{\beta} + \frac{1}{\alpha\beta} \quad (3)$$

Where the parameters α, and β can be expressed as the following formulas [4]:

$$\alpha = \left[\exp\left\{ \frac{0.49\sigma^2}{\left(1 + 0.18d^2 + 0.56\,\sigma^{12/5}\right)^{7/6}} \right\} - 1 \right]^{-1} \quad (4)$$

$$\beta = \left[\exp\left\{ \frac{0.51\sigma^2 + \left(1 + 0.69\sigma^{12/5}\right)^{-5/6}}{\left(1 + 0.9\,d^2 + 0.62 d^2\,\sigma^{12/5}\right)} \right\} - 1 \right]^{-1} \quad (5)$$

Where the laser intensity fluctuations σ can be given by the following formula [5]:

$$\sigma = \sqrt{0.5 C_n^2 \left(\frac{2\pi}{\lambda}\right)^{7/6} L^{11/6}} \quad (6)$$

Where L is the propagation length, and C_n^2 is the refractive index structure turbulence in $m^{-2/3}$ and the d parameter is equal to $d=\pi D^2/2\lambda L$, here D is the receiver diameter. There are many different types of modulation schemes which are suitable for FSO communication systems such as on-off keying (OOK), N-PPM, M-PAM, and H-QAM. Since the average emitted optical power is always limited, the performance of modulation techniques is often compared in terms of the average received optical power required to achieve a desired BER at a given data rate. It is very desirable for the modulation scheme to be power efficient, but this is however not the only deciding factor in the choice of a modulation technique. The probability of error for NRZ-OOK and RZ-OOK coded optical data, detected with a photodiode, can be expressed as a function of the signal to noise ratio (SNR) as in [6].

$$BER_{NRZ-OOK} = 0.5\, erfc\left(\frac{0.5\sqrt{SNR}}{\sqrt{2}}\right) \quad (7)$$

$$BER_{NR-OOK} = 0.5\, erfc\left(\frac{\sqrt{SNR}}{2}\right) \quad (8)$$

Since the required bandwidth for NRZ-OOK is equal to the bit rate, i.e., R_b=B, so the theoretical bandwidth efficiency for this modulation scheme is unity. While the required bandwidth for RZ-OOK is double the required bandwidth for NRZ-OOK [1], then it is equal to double the bit rate, i.e., R_b=2B. So, RZ-OOK has a theoretical bandwidth efficiency of 0.5 bps/Hz.

II. 1. Pulse Position Modulation (N-PPM)

In this modulation scheme, each pulse of a laser can be used to represent one or more bits of information by its position in time relative to the start of a symbol whose duration is identical to that of information bits it contains. And the great advantage of PPM scheme is the elimination of decision threshold dependence on the input power [7-11]. Since N is the possible pulse positions code for K_1 bits of information in PPM scheme, and the bit rate can be expressed as follows [12]:

$$R_{b(PPM)} = \frac{B \log_2 N}{N} \quad (9)$$

For Gaussian noise, the BER for N-PPM scheme can be expressed as [13]:

$$BER_{PPM} = 0.5\, erfc\left(\frac{0.5}{\sqrt{2}} SNR\left(\frac{N}{2}\log_2 N\right)\right) \quad (10)$$

The bandwidth efficiency η_{PPM} for N-PPM can be expressed as a function of as follows:

$$\eta_{PPM} = \frac{\log_2 N}{N} \quad (11)$$

As well as the transmission data rate and bandwidth efficiency for differential PPM (DPPM) and differential amplitude PPM (DAPPM) can be given by the following formulas [14]:

$$R_{b(DPPM)} = \frac{\left(2^N + 1\right)B}{2\,N} \quad (12)$$

$$R_{b(DAPPM)} = \frac{\left(2^N + M\right)B}{2\,NM} \quad (13)$$

$$\eta_{DPPM} = \frac{\left(2^N + 1\right)}{2\,N} \quad (14)$$

$$\eta_{DPPM} = \frac{\left(2^N + M\right)}{2\,NM} \quad (15)$$

Where M is the number of amplitude levels.

II. 2. Pulse Amplitude Modulation (M-PAM)

Since M is the possible pulse amplitudes code for K_2 bits of information in M-PAM, i.e., $M=2^{K2}$, and the transmission bit rate can be expressed as follows [15, 16]:

$$R_{b(PAM)} = B \log_2 M \quad (16)$$

It is a form of signal modulation where the message information is encoded in the amplitude of a series of signal pulses; and the BER for M-PAM scheme can be expressed as follows [17]:

$$BER_{PAM} = 0.5 erfc\left(\frac{\sqrt{SNR \log_2 M}}{2\sqrt{2}(M-1)}\right) \quad (17)$$

As well as he bandwidth efficiency η_{PAM} for M-PAM can be expressed as a function of as follows:

$$\eta_{PAM} = \log_2 M \quad (18)$$

II. 3. Quadrature Amplitude Modulation (H-QAM)

When two baseband signals, each of bandwidth B Hz, can be transmitted simultaneously over a bandwidth 2B by using QAM Modulation. Now we consider data symbols which comprise $\log_2$ H data symbols which have been mapped to one of the H phases on each carrier signal m(t). So the conditional bit rate and BER expressions for H-QAM can be given by [18]:

$$R_{b(QAM)} = 2B \log_2 H \quad (19)$$

$$BER_{QAM} = \frac{2\left(1-\frac{1}{\sqrt{M}}\right)}{\log_2 M} erfc\left(\frac{3 \log_2 M (SNR)}{2(M-1)}\right) \quad (20)$$

As well as he bandwidth efficiency η_{QAM} for H-QAM can be expressed as a function of as follows:

$$\eta_{QAM} = 2\log_2 H \quad (21)$$

The required minimum detectable received power for FSO communication systems under various modulation schemes can readily be derived from the BER expression for all modulation schemes and can be [17, 18]:

$$P_R = \frac{\sigma \sqrt{SNR}}{R} \quad (22)$$

Where R is the photo detector sensitivity or responsitivity.

III. Simulation Results and Performance Evaluation

The comparative study of the N-PPM and M-PAM, DPPM, and DAPPM schemes are discussed, N-PPM scheme offered improved performance. For FSO communication systems, although the power efficiency is inferior to N-PPM scheme, OOK modulation scheme is more commonly used due to its efficient bandwidth usage, but M-PAM is the bandwidth efficient modulation scheme, while N-PPM is the power efficient modulation scheme for more number of bits can be sent, and it may be able to improve performance by increasing the number of bits in N-PPM scheme. These modulation techniques are deeply investigated over wide range of the affecting parameters as listed in Table 1.

Table 1: List of simulation parameters used in free space optics systems [3, 7, 12, 14, 18].

Operating parameter	Value and unit
Laser wavelength, λ	850 nm ≤ λ ≤1550 nm
Detector quantum efficiency, η	0.85
Signal power, P_{S0}	100 mW
Mean signal power, P_S	20 mW
Bandwidth, B	2.5 Gb/sec ≤ B ≤ 40 Gb/sec
Propagation length, L	100 m ≤ L ≤ 1000 m
Refractive index turbulence, C_n^2	10^{-17} $m^{-2/3}$ ≤ C_n^2 ≤ 10^{-13} $m^{-2/3}$
Pulse amplitudes code, M	4 ≤ M ≤ 64
Pulse positions code, N	4 ≤ N ≤ 64
Receiver diameter, D	5 ≤ D, cm ≤ 20
Signal to noise ratio, SNR	5 dB ≤ SNR ≤ 20 dB
Quadrate amplitudes code, H	4 ≤ H ≤ 64
Si APD responsitivity, R_{Si} (1550 nm)	35
Ge APD responsitivity, R_{Ge} (1550 nm)	10
InGaAs APD responsitivity, R_{InGaAs} (1550 nm)	0.85
Si PIN responsitivity, R_{Si} (1550 nm)	0.65
Ge PIN responsitivity, R_{Ge} (1550 nm)	0.68
In GaAs PIN responsitivity, R_{InGaAs} (1550 nm)	0.71

Based on the modeling equations analysis and the assumed set of the operating parameters as shown in Table 1. The following facts are assured as shown in the series of Figs. (1-29):

i) Fig. 1 has assured that signal to noise ratio increases with increasing operating laser signal wavelength and decreasing propagation length.

ii) Figs. (2-4) have indicated that signal to noise ratio increases with increasing receiver aperture diameter and decreasing transmitted bandwidth for different turbulence channels. It is observed that with strong turbulence channel has presented the lowest signal to noise ratio in compared with other turbulence channels.

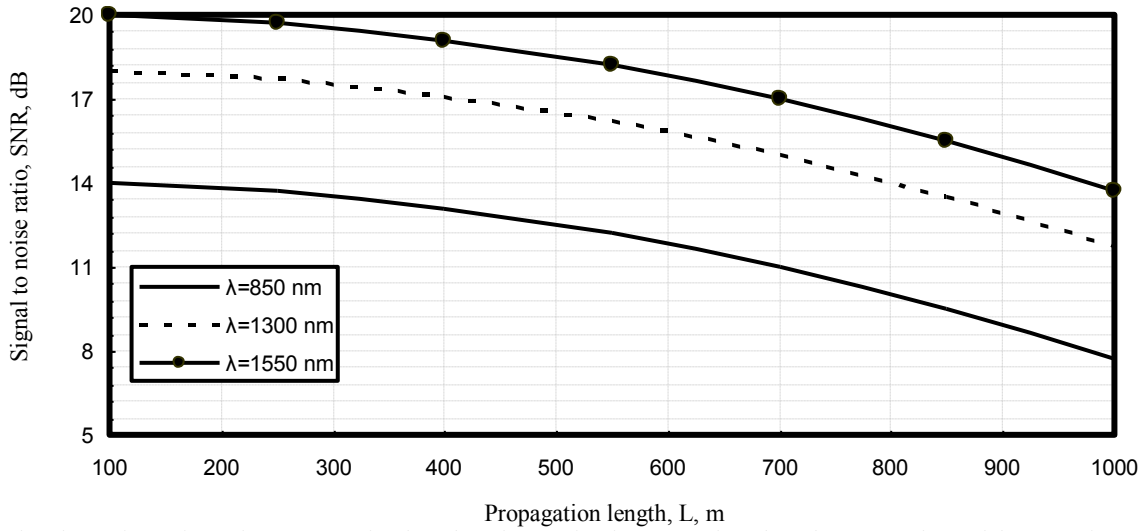

Fig. 1. Signal to noise ratio against propagation length and operating laser wavelength at the assumed set of the operating parameters.

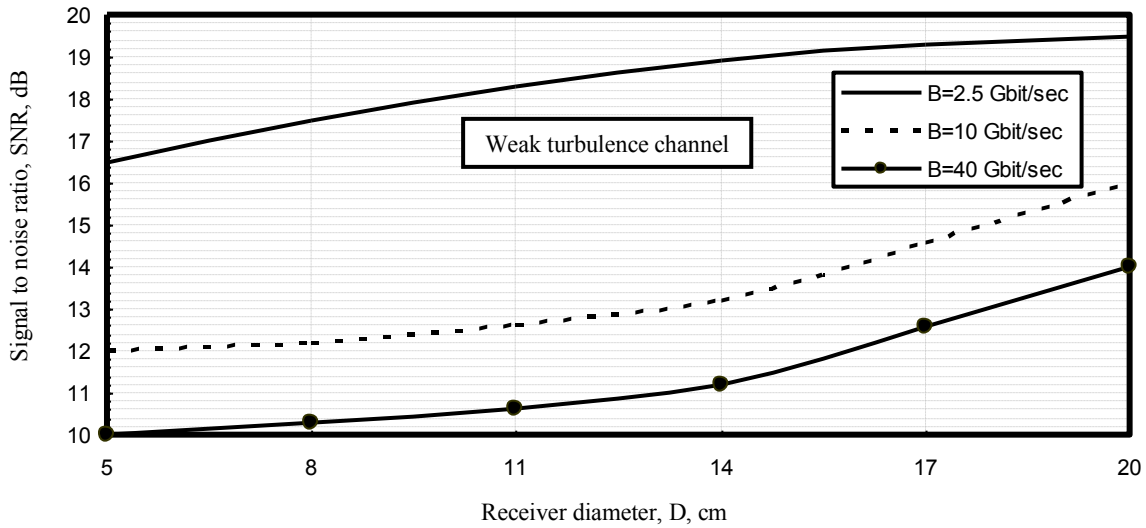

Fig. 2. Signal to noise ratio versus receiver diameter and transmission bandwidth with third operating laser wavelength (λ=1550 nm) with weak refractive index structure turbulence strength (C_n^2 x10^{-17}, $m^{-2/3}$), average propagation length at the assumed set of the operating parameters.

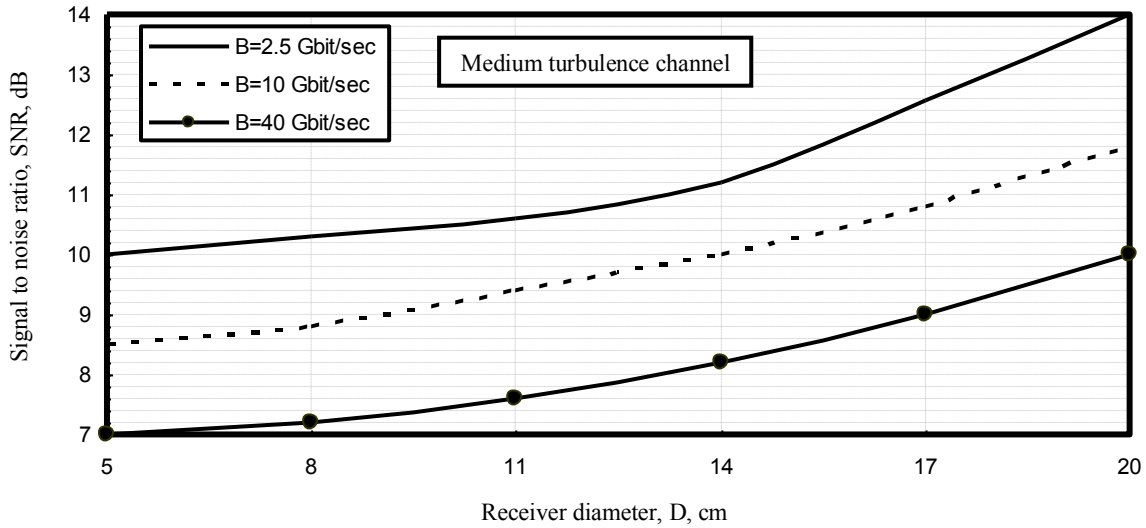

Fig. 3. Signal to noise ratio versus receiver diameter and transmission bandwidth with third operating laser wavelength (λ=1550 nm) with medium refractive index structure turbulence strength (C_n^2 x10^{-15}, $m^{-2/3}$), average propagation length at the assumed set of the operating parameters.

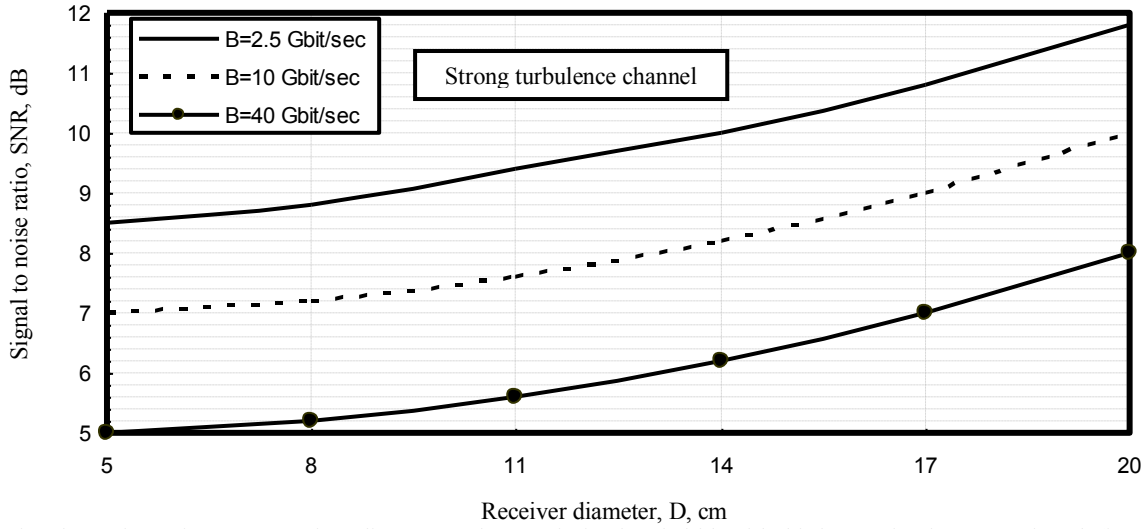

Fig. 4. Signal to noise ratio versus receiver diameter and transmission bandwidth with third operating laser wavelength (λ=1550 nm) with strong refractive index structure turbulence strength (C_n^2 x10^{-13}, m-$^{2/3}$), average propagation length at the assumed set of the operating parameters.

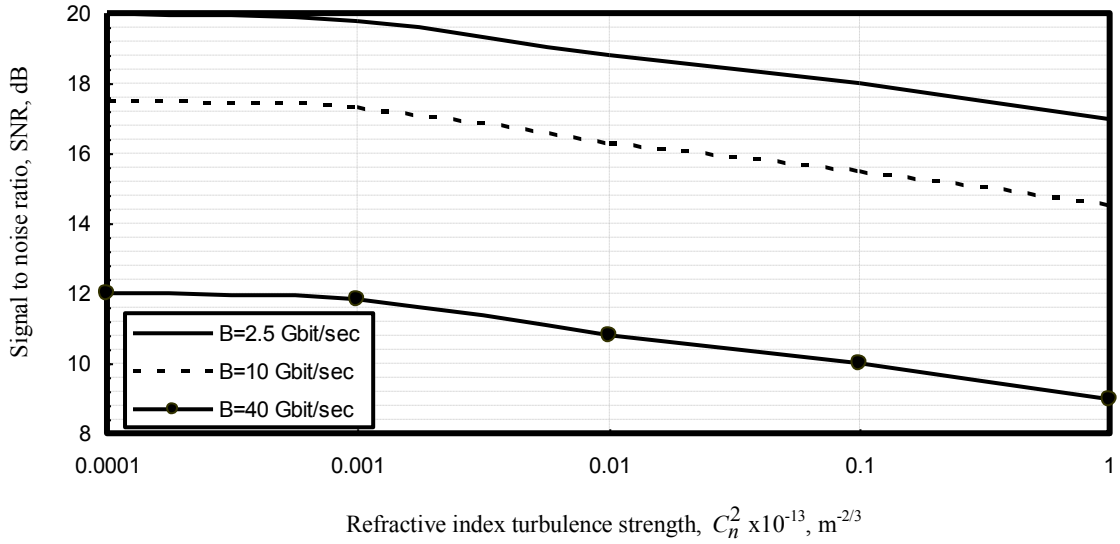

Fig. 5. Signal to noise ratio in relation to refractive index structure turbulence strength and transmission bandwidth with third operating laser wavelength (λ=1550 nm) and propagation length (L=100 m) at the assumed set of the operating parameters.

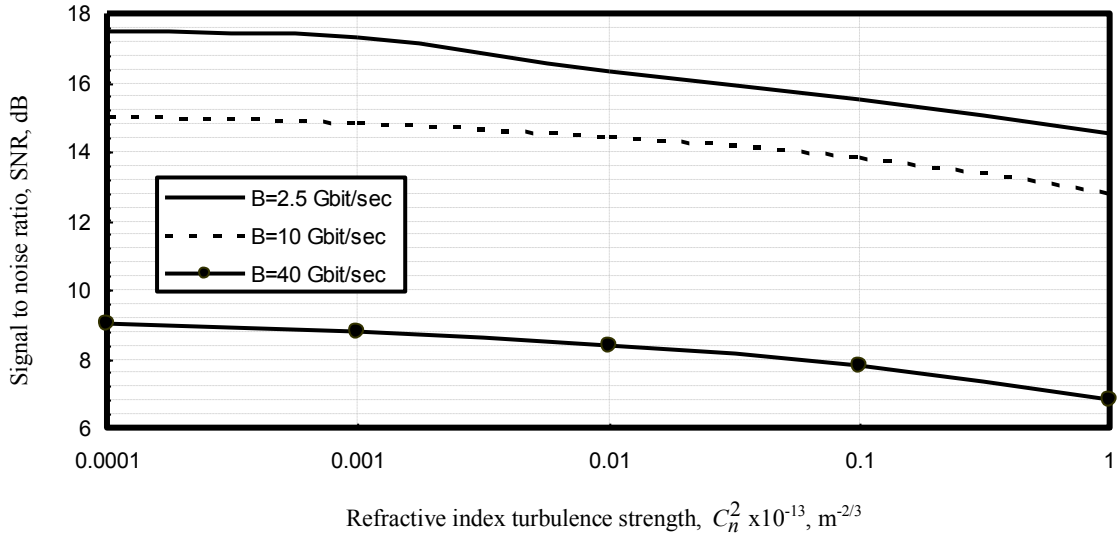

Fig. 6. Signal to noise ratio in relation to refractive index structure turbulence strength and transmission bandwidth with third operating laser wavelength (λ=1550 nm) and propagation length (L=550 m) at the assumed set of the operating parameters.

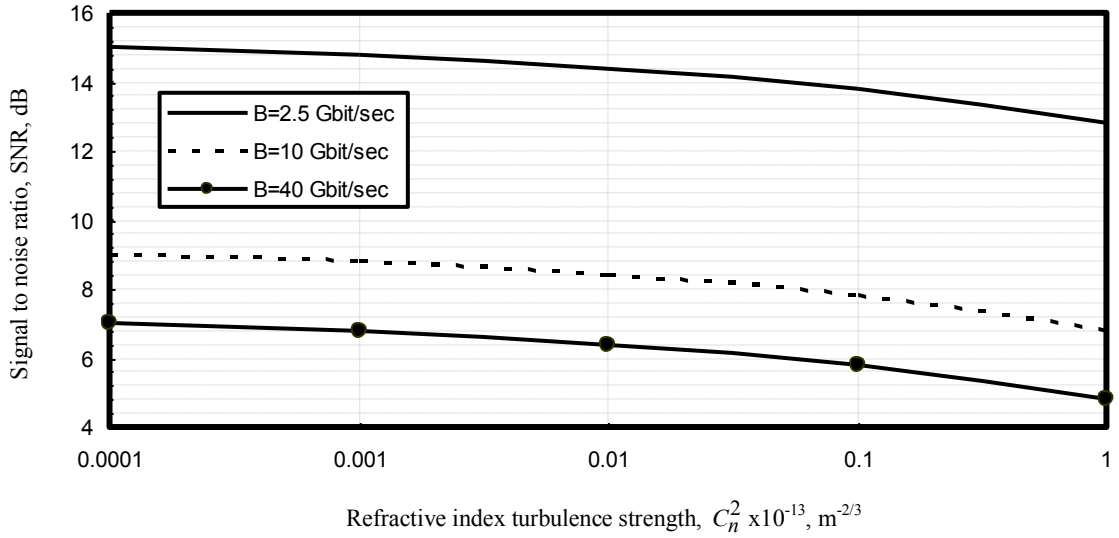

Fig. 7. Signal to noise ratio in relation to refractive index structure turbulence strength and transmission bandwidth with third operating laser wavelength (λ=1550 nm) and propagation length (L=1000 m) at the assumed set of the operating parameters.

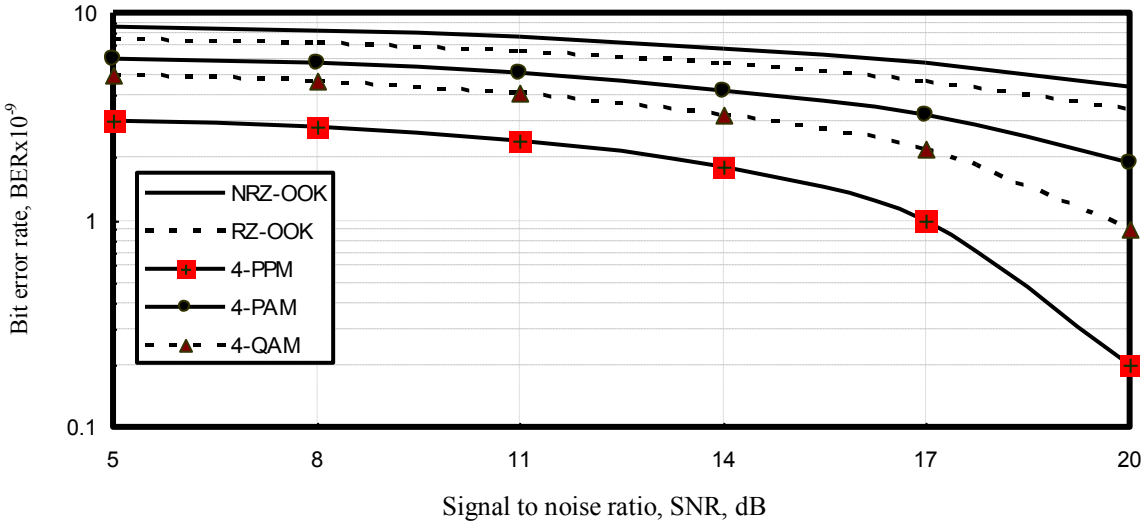

Fig. 8. Bit error rate in relation to signal to noise ratio for different modulation techniques with four quantization levels at the assumed set of the operating parameters.

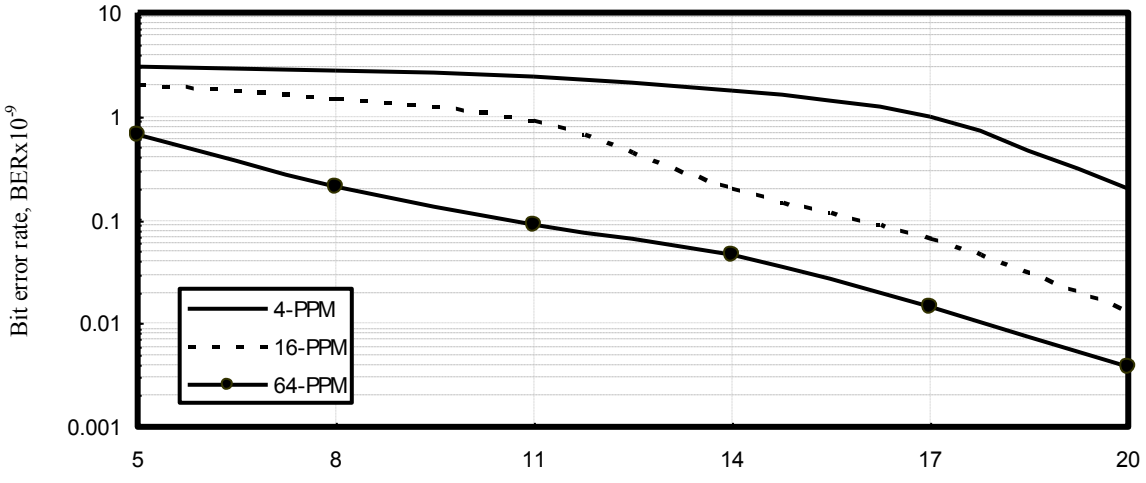

Fig. 9. Bit error rate in relation to signal to noise ratio for pulse position modulation technique with different position levels at the assumed set of the operating parameters.

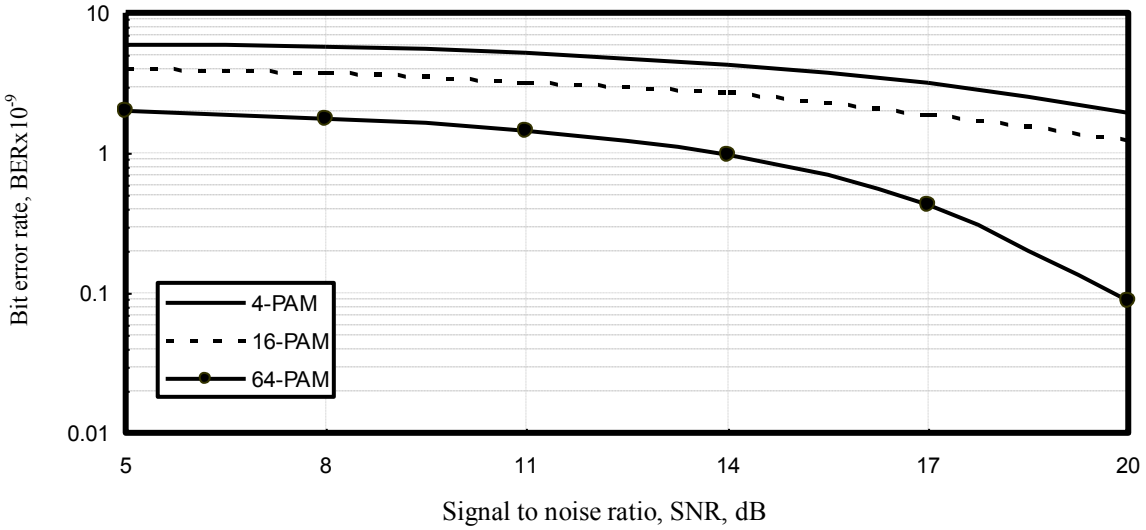

Fig. 10. Bit error rate in relation to signal to noise ratio for pulse amplitude modulation technique with different amplitude levels at the assumed set of the operating parameters.

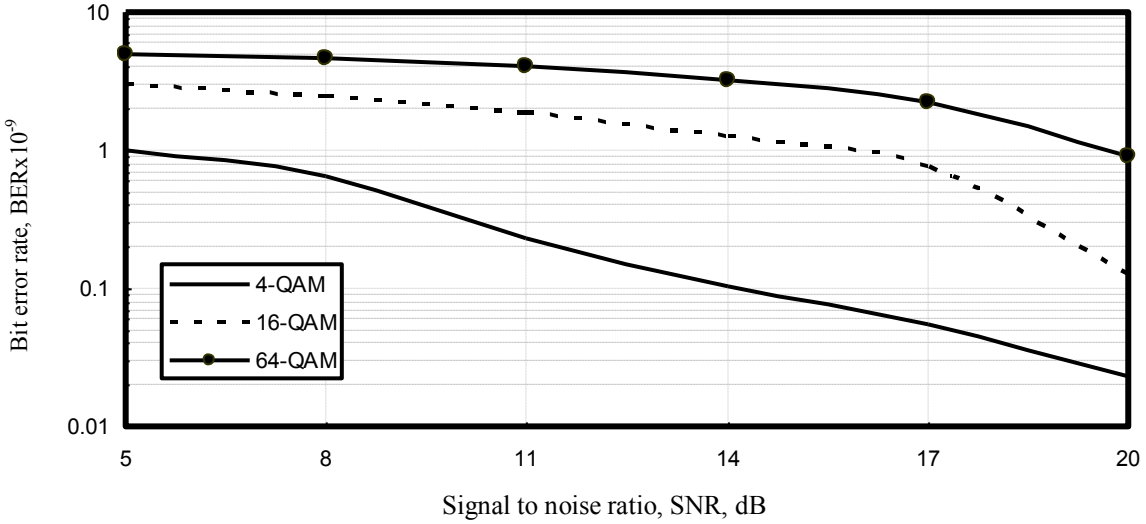

Fig. 11. Bit error rate in relation to signal to noise ratio for quadature amplitude modulation technique with different quadrate amplitude levels at the assumed set of the operating parameters.

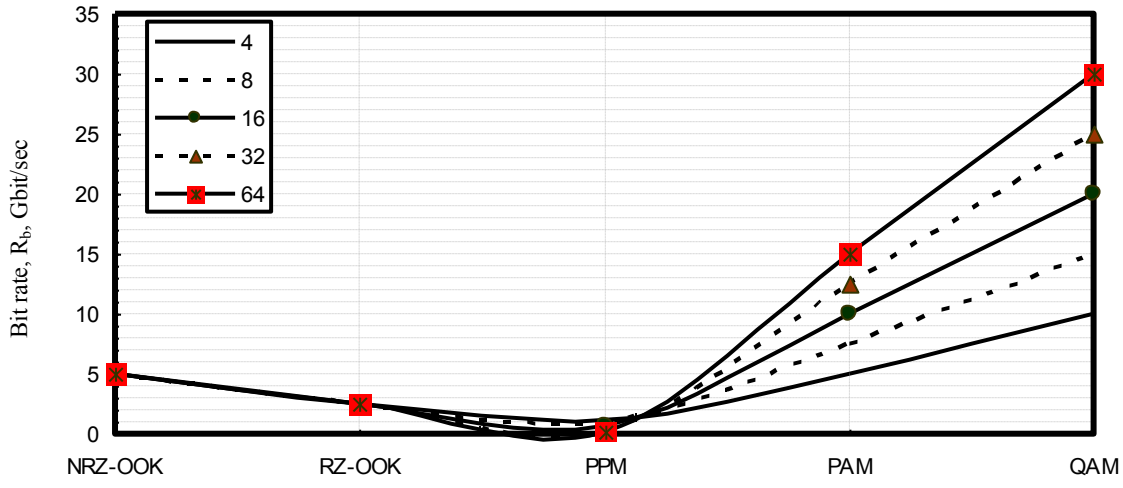

Fig. 12. Transmission bit rate against different modulation techniques and different number of quantization coding levels with required bandwidth (B=2.5 Gbit/sec) at the assumed set of the operating parameters.

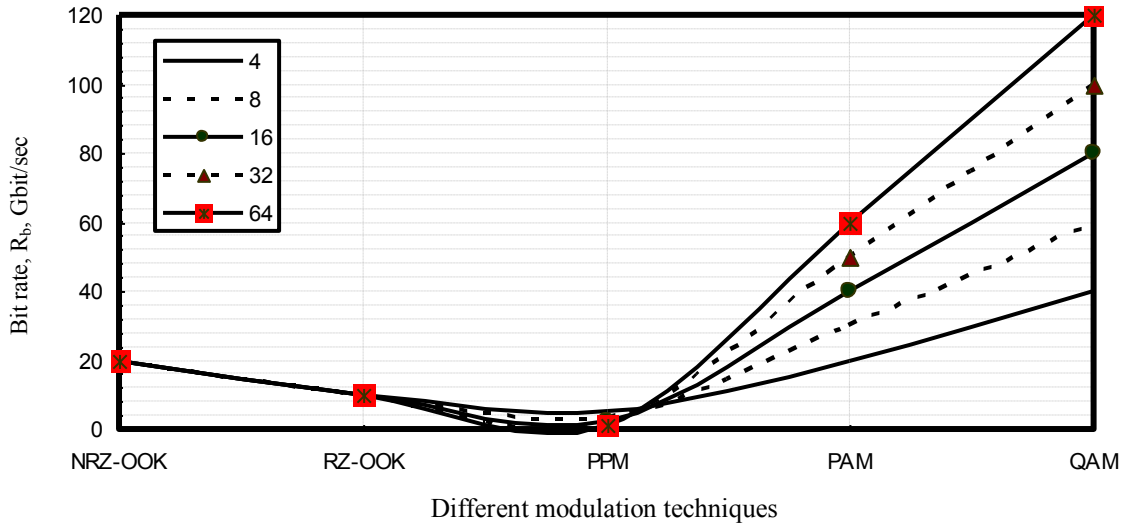

Fig. 13. Transmission bit rate against different modulation techniques and different number of quantization coding levels with required bandwidth (B=10 Gbit/sec) at the assumed set of the operating parameters.

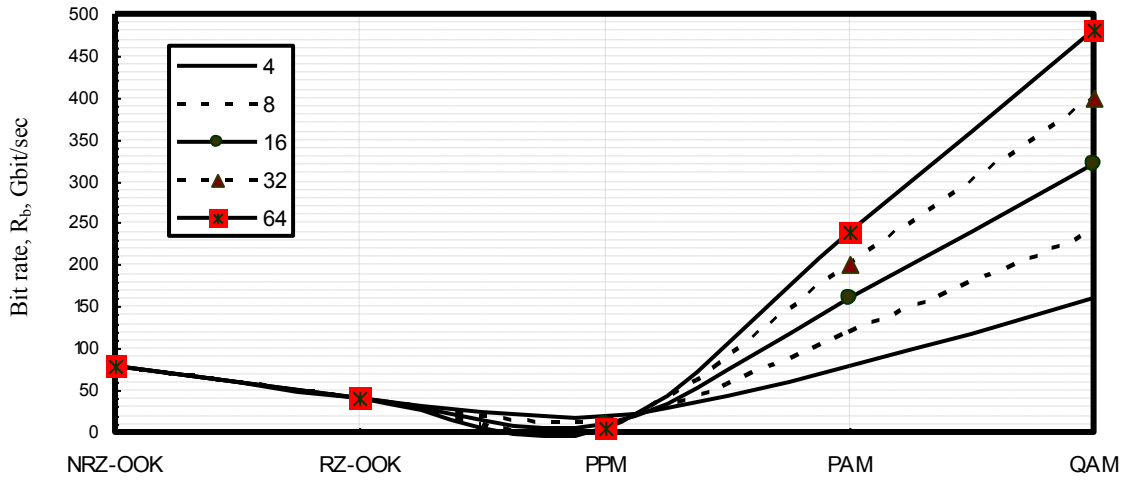

Fig. 14. Transmission bit rate against different modulation techniques and different number of quantization coding levels with required bandwidth (B=40 Gbit/sec) at the assumed set of the operating parameters.

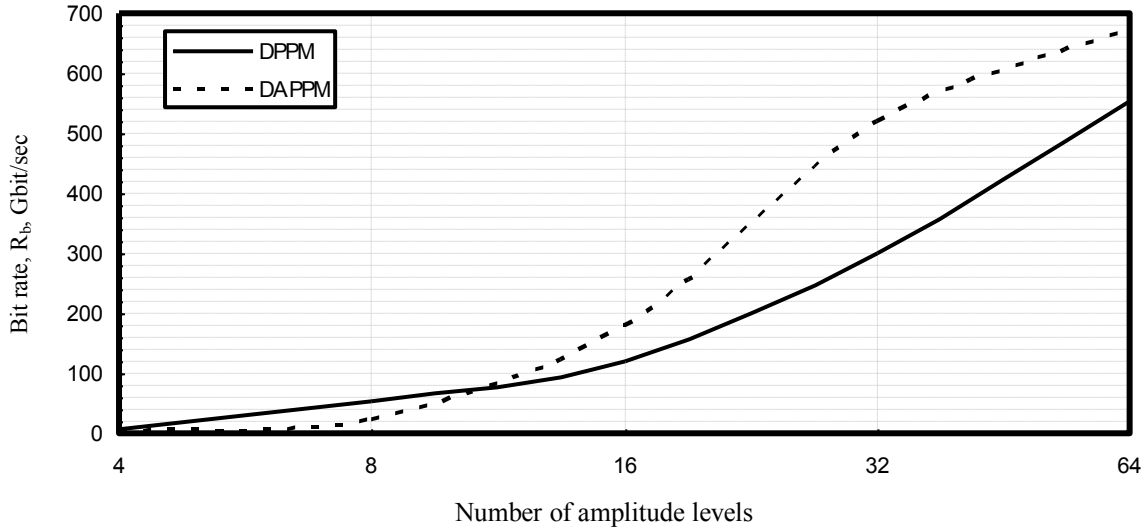

Fig. 15. Transmission bit rate against different number of quantization amplitude and position coding levels at the assumed set of the operating parameters.

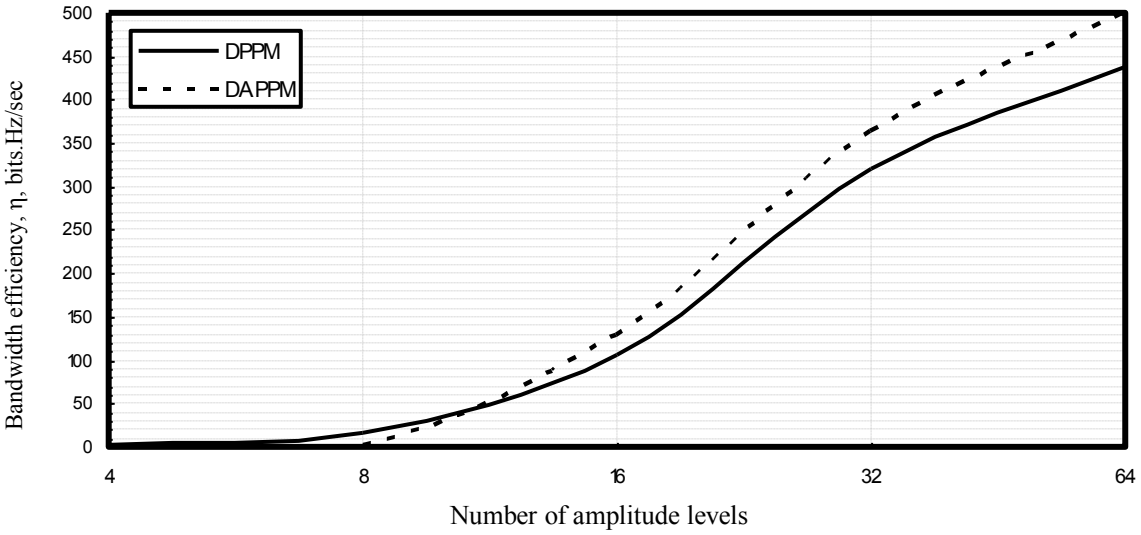

Fig. 16. Bandwidth efficiency against different number of quantization amplitude and position coding levels at the assumed set of the operating parameters.

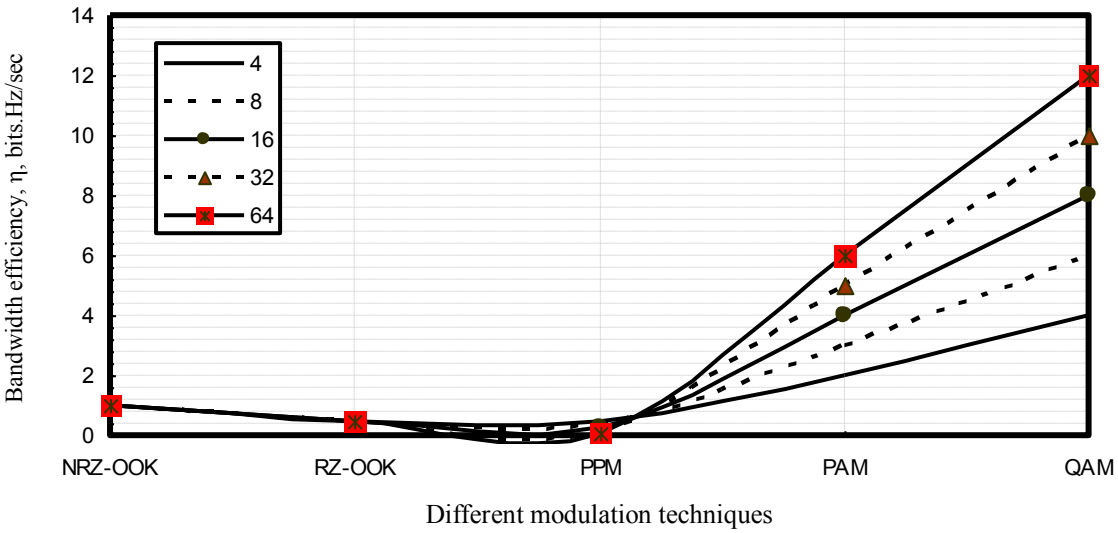

Fig. 17. Bandwidth efficiency against different modulation techniques and different number of quantization coding levels at the assumed set of the operating parameters.

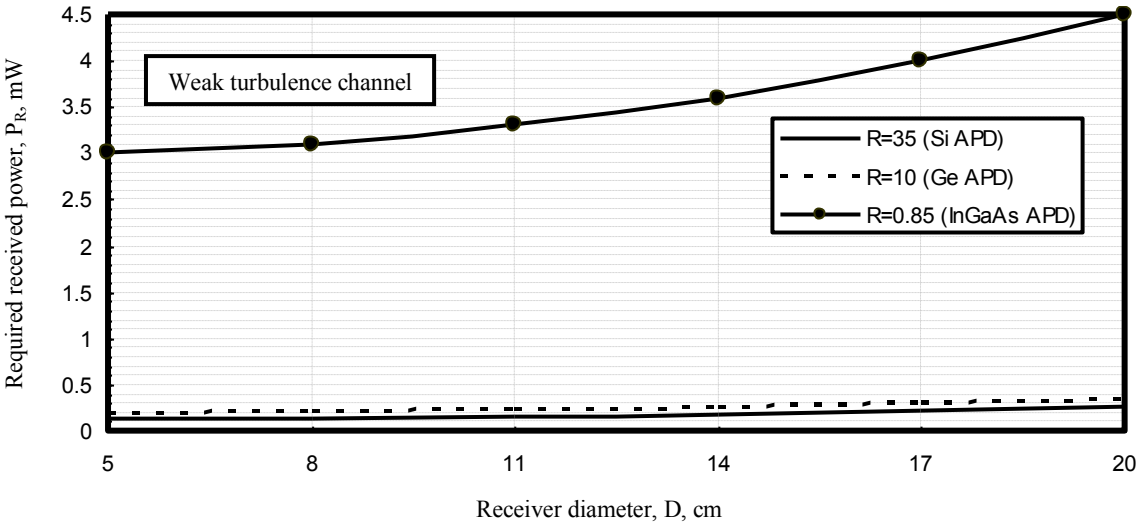

Fig. 18. Required minimum detectable received power against receiver diameter and different avalanche photodiode receivers with average transmission bandwidth, third operating laser wavelength (λ=1550 nm) within weak refractive index structure turbulence strength (C_n^2 x10^{-17}, $m^{-2/3}$), and average propagation length at the assumed set of the operating parameters.

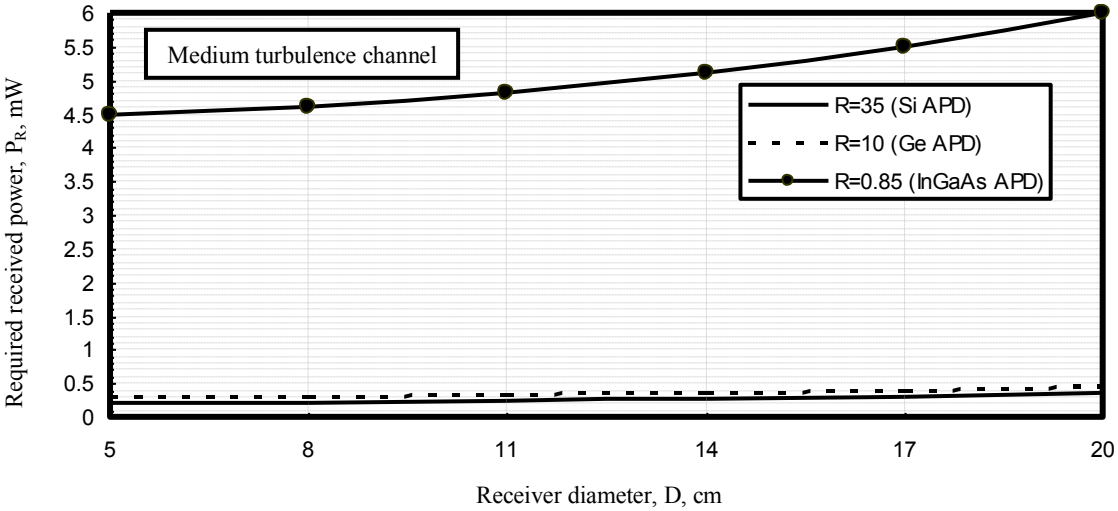

Fig. 19. Required minimum detectable received power against receiver diameter and different avalanche photodiode receivers with average transmission bandwidth, third operating laser wavelength (λ=1550 nm) within medium refractive index structure turbulence strength (C_n^2 x10^{-15}, $m^{-2/3}$), and average propagation length at the assumed set of the operating parameters.

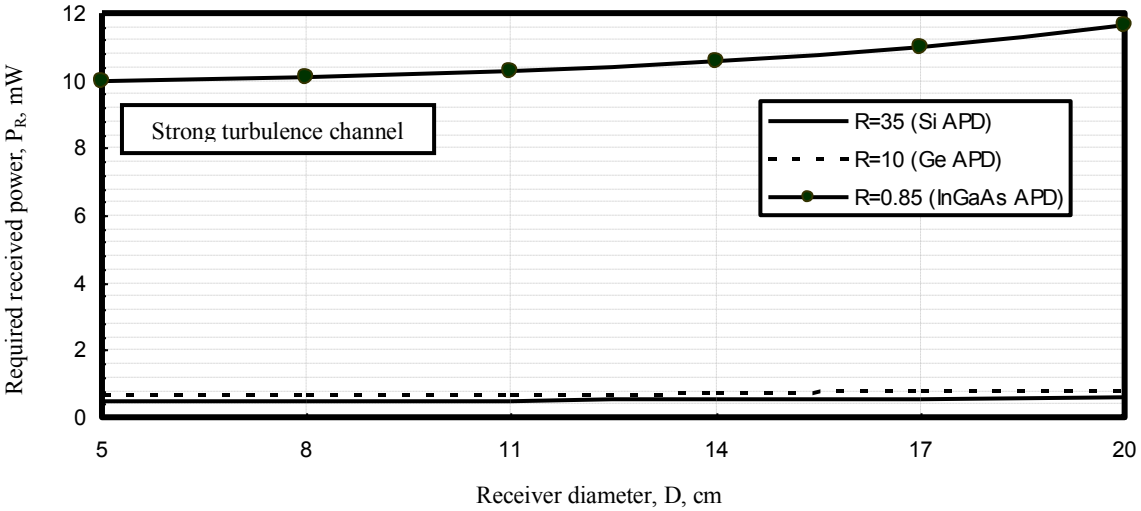

Fig. 20. Required minimum detectable received power against receiver diameter and different avalanche photodiode receivers with average transmission bandwidth, third operating laser wavelength (λ=1550 nm) within strong refractive index structure turbulence strength (C_n^2 x10^{-13}, $m^{-2/3}$), and average propagation length at the assumed set of the operating parameters.

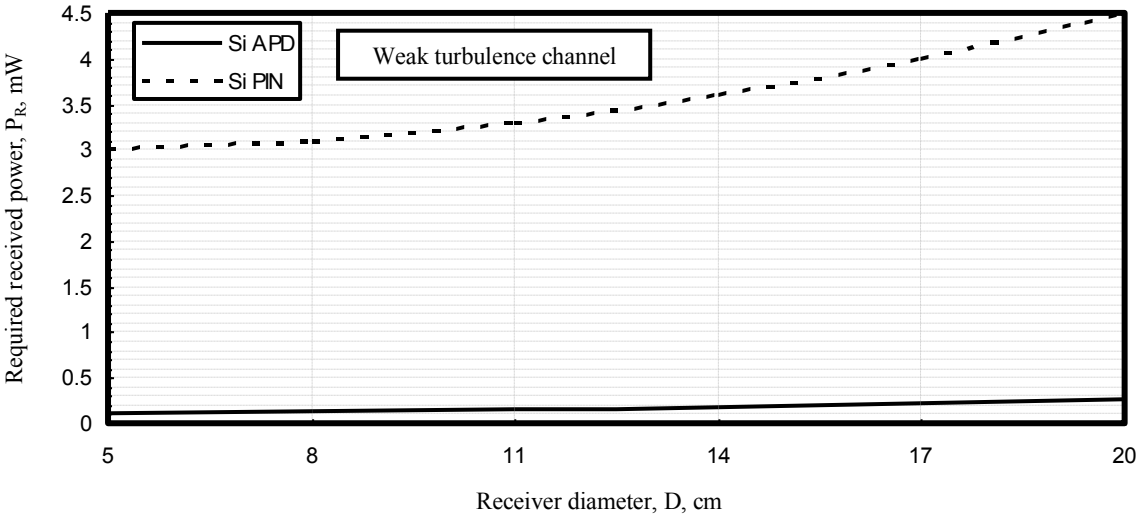

Fig. 21. Required minimum detectable received power against receiver diameter and different silicon photodiode receivers types with average transmission bandwidth, third operating laser wavelength (λ=1550 nm) within weak refractive index structure turbulence strength (C_n^2 x10^{-17}, $m^{-2/3}$), and average propagation length at the assumed set of the operating parameters.

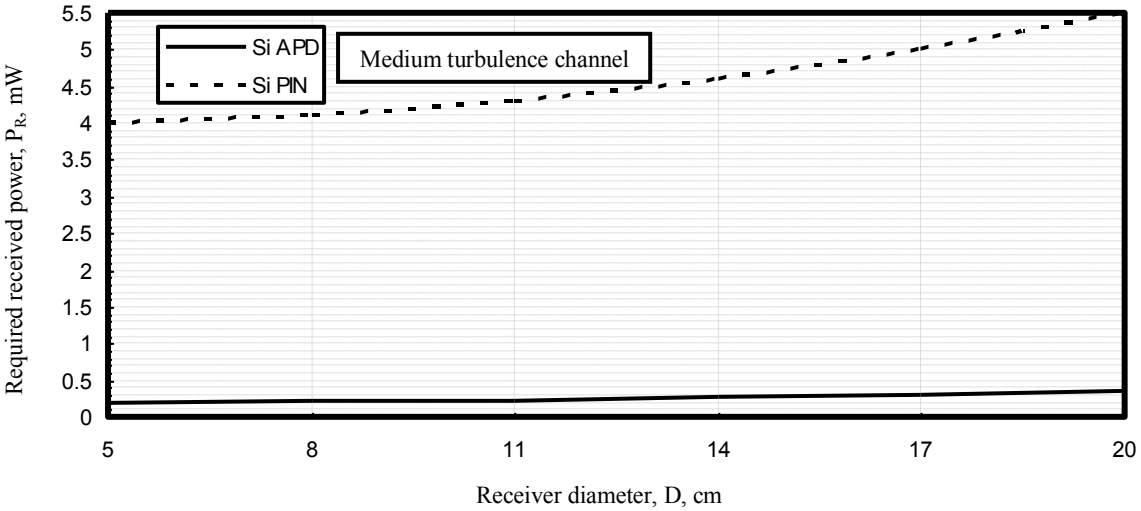

Fig. 22. Required minimum detectable received power against receiver diameter and different silicon photodiode receivers types with average transmission bandwidth, third operating laser wavelength (λ=1550 nm) within medium refractive index structure turbulence strength (C_n^2 x10^{-15}, $m^{-2/3}$), and average propagation length at the assumed set of the operating parameters.

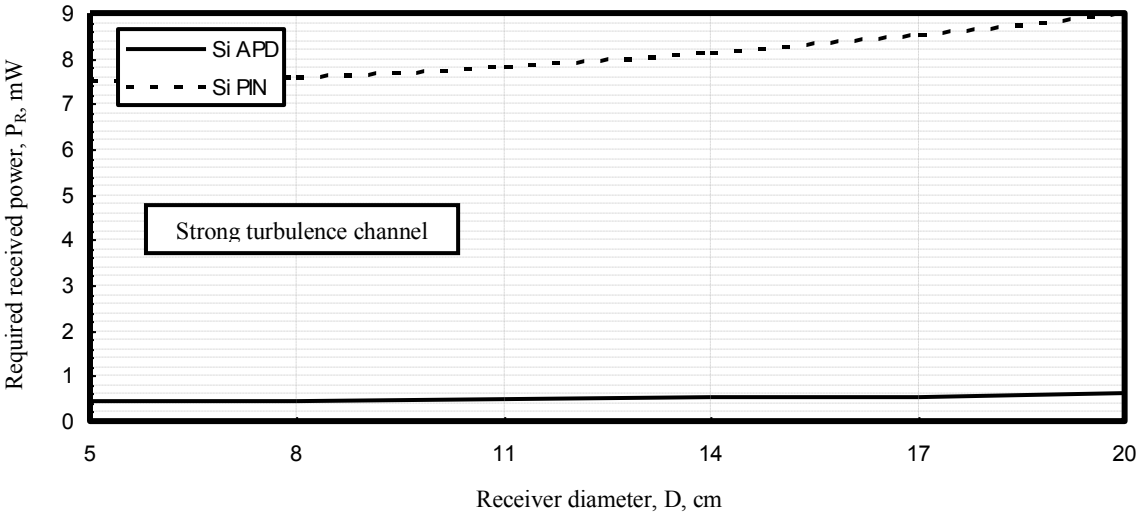

Fig. 23. Required minimum detectable received power against receiver diameter and different silicon photodiode receivers types with average transmission bandwidth, third operating laser wavelength (λ=1550 nm) within strong refractive index structure turbulence strength (C_n^2 x10^{-13}, $m^{-2/3}$), and average propagation length at the assumed set of the operating parameters.

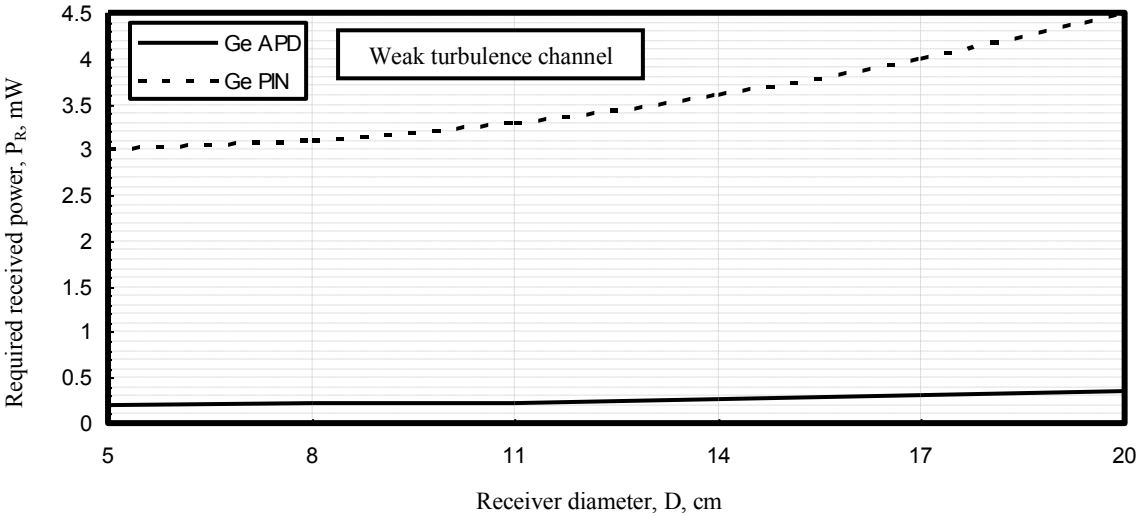

Fig. 24. Required minimum detectable received power against receiver diameter and different germanium photodiode receivers types with average transmission bandwidth, third operating laser wavelength (λ=1550 nm) within weak refractive index structure turbulence strength (C_n^2 x10^{-17}, $m^{-2/3}$), and average propagation length at the assumed set of the operating parameters.

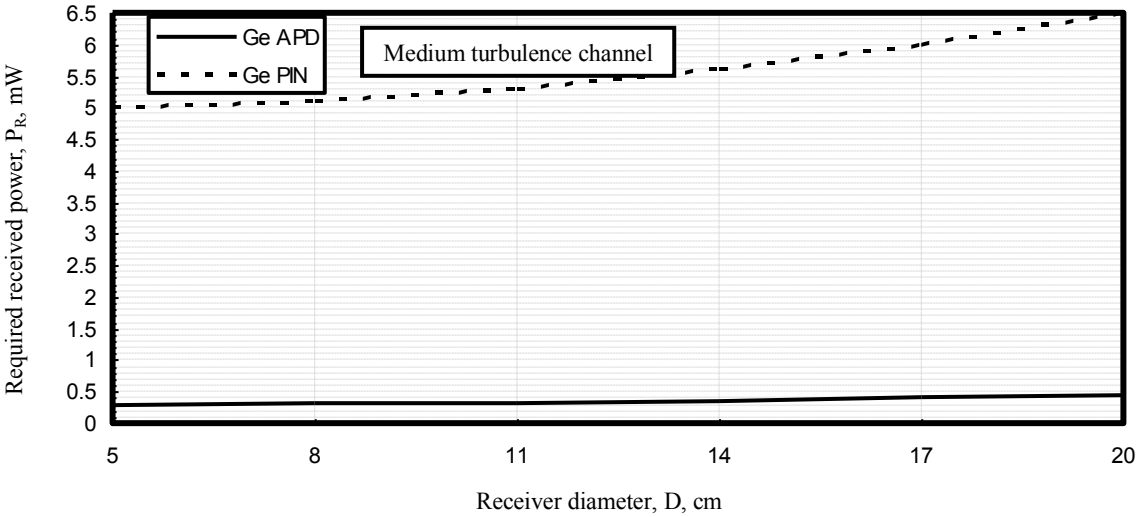

Fig. 25. Required minimum detectable received power against receiver diameter and different germanium photodiode receivers types with average transmission bandwidth, third operating laser wavelength (λ=1550 nm) within medium refractive index structure turbulence strength (C_n^2 x10^{-15}, $m^{-2/3}$), and average propagation length at the assumed set of the operating parameters.

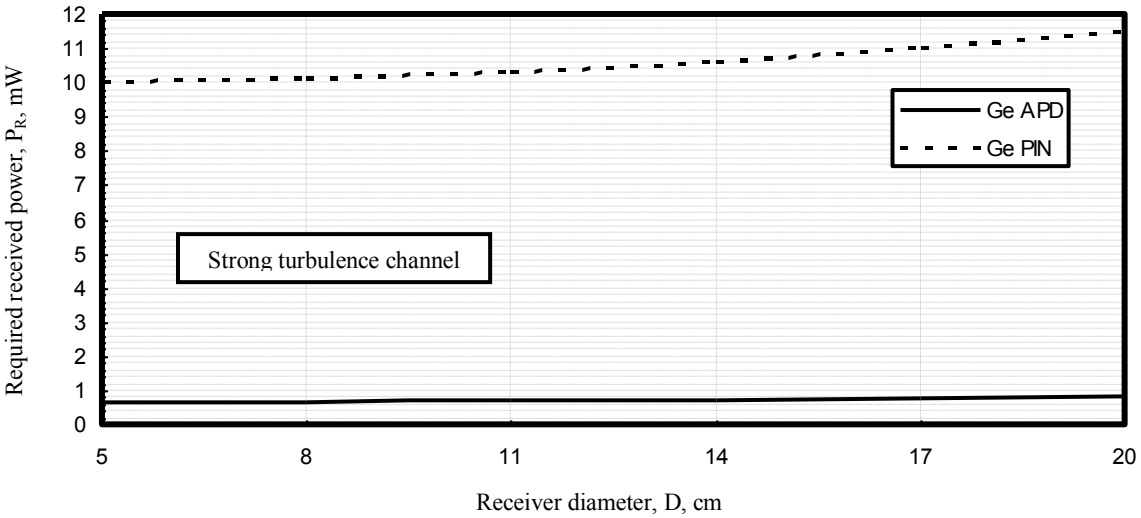

Fig. 26. Required minimum detectable received power against receiver diameter and different germanium photodiode receivers types with average transmission bandwidth, third operating laser wavelength (λ=1550 nm) within strong refractive index structure turbulence strength (C_n^2 x10^{-13}, $m^{-2/3}$), and average propagation length at the assumed set of the operating parameters.

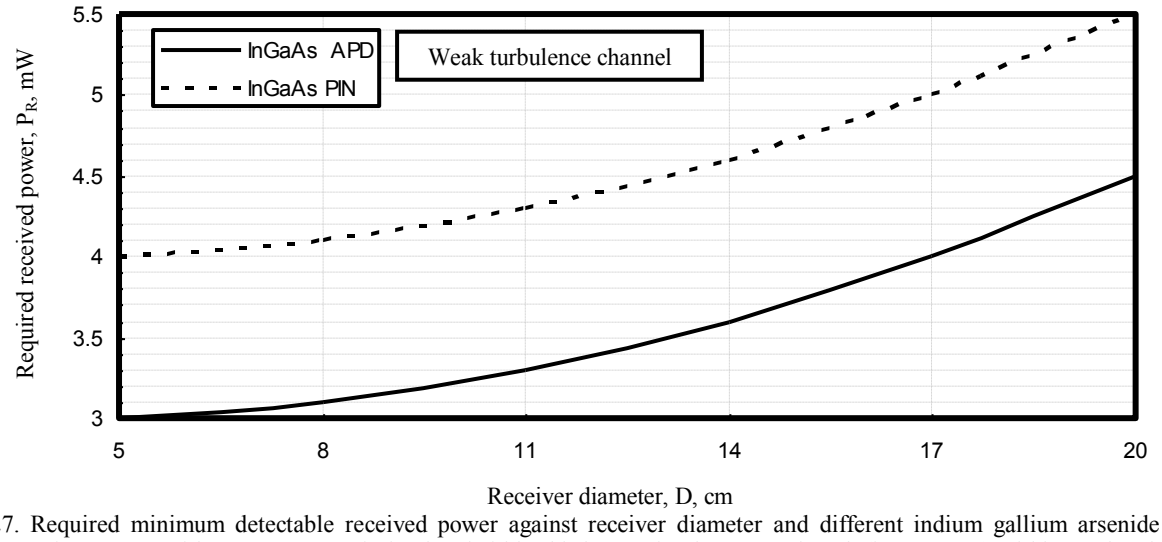

Fig. 27. Required minimum detectable received power against receiver diameter and different indium gallium arsenide photodiode receivers types with average transmission bandwidth, third operating laser wavelength (λ=1550 nm) within weak refractive index structure turbulence strength (C_n^2 x10^{-17}, $m^{-2/3}$), and average propagation length at the assumed set of the operating parameters.

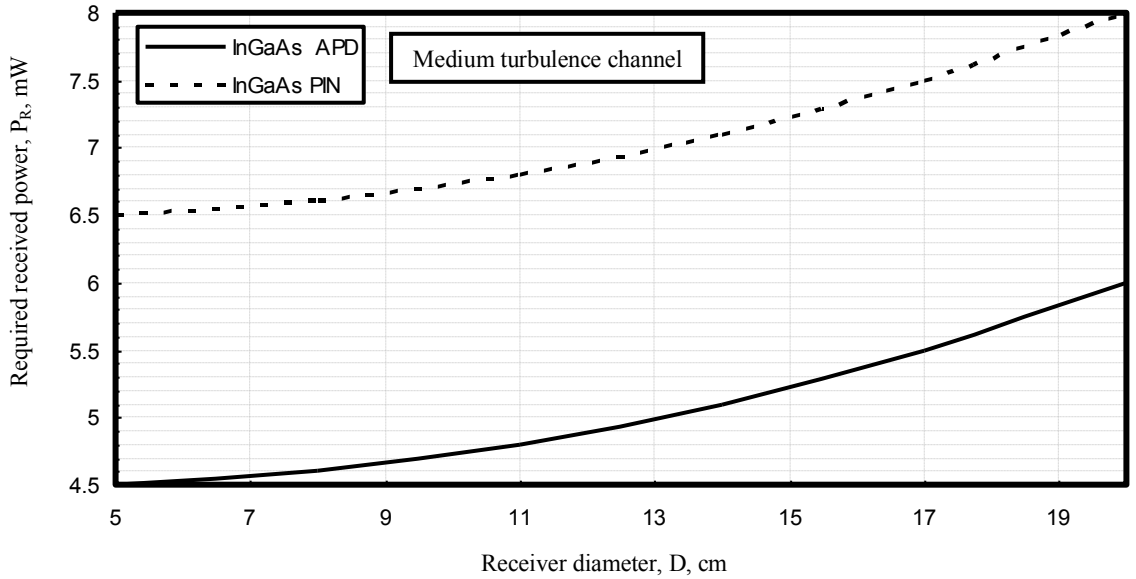

Fig. 28. Required minimum detectable received power against receiver diameter and different indium gallium arsenide photodiode receivers types with average transmission bandwidth, third laser wavelength (λ=1550 nm) within medium refractive index structure turbulence strength (C_n^2 x10^{-15}, $m^{-2/3}$), and average propagation length at the assumed set of the operating parameters.

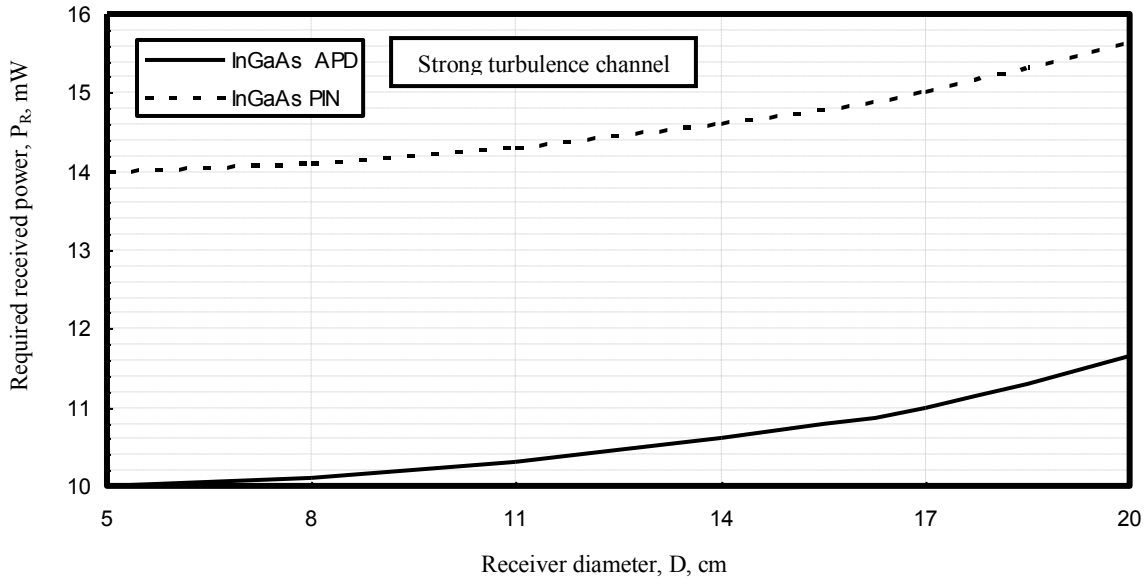

Fig. 29. Required minimum detectable received power against receiver diameter and different indium gallium arsenide photodiode receivers types with average transmission bandwidth, third operating laser wavelength (λ=1550 nm) within strong refractive index structure turbulence strength (C_n^2 x10^{-13}, $m^{-2/3}$), and average propagation length at the assumed set of the operating parameters.

iii) Figs. (5-7) have assured that signal to noise ratio increases with decreasing transmitted bandwidth, propagation length and refractive index structure turbulence strength at the assumed set of list operating parameters.

iv) Fig. 8 has indicated that bit error rate decreases with increasing signal to noise ratio for different modulation techniques under study considerations. It is observed that PPM modulation technique has presented the lowest bit error rate in compared with other modulation techniques under the same operating conditions.

v) Figs. (9, 10) have assured that bit error rates decrease with increasing both signal to noise ratio and coding levels for both PPM and PAM.

vi) Fig. 11 has proved that bit error rate decreases with increasing signal to noise ratio and decreasing coding levels for QAM.

vii) As shown in figs. (12-14) have indicated that with increasing transmitted bandwidth and number of coding levels, this results in increasing of transmission bit rate for different modulation techniques expect for NRZ-OOK, RZ-OOK which are kept constant, and QAM which decreases its values under the same operating conditions.

viii) As shown in figs. (15, 16) have assured that DAPPM has presented the highest both transmission bit rate and bandwidth efficiency than DPPM under the same operating conditions.

ix) Fig. 17 has indicated that with increasing number of coding levels, this results in increasing of bandwidth efficiency for different modulation techniques expect for NRZ-OOK, RZ-OOK which are kept constant under the same operating conditions.

x) As shown in figs. (18-20) have assured that required minimum detectable received signal power increases

with increasing receiver aperture diameter, and decreasing detector receiver responsitivity and with different channel turbulence strength. It is observed that the increased required received signal power in the case of strong turbulence channel in compared with other turbulence channels.

xi) AS shown in the series of figs. (21-29) have indicated that required minimum detectable received signal power increases with increasing receiver aperture diameter, and different photodiode receivers types from Silicon, Ge to InGaAs and with different channel turbulence strength. It is observed that the increased required received signal power in the case of strong turbulence channel in compared with other turbulence channels.

IV. CONCLUSIONS

In a summary, this paper has presented different modulation techniques for free space optical communication systems transmission efficiency enhancement and transmission capacity estimation in weak and strong turbulence channels. It is theoretically found that PPM modulation technique has presented the highest signal to noise ratio and the lowest bit error rates in compared with other modulation techniques under the same operating worst conditions in both weak and strong turbulence channel. It is indicated that the decreased propagation length, refractive index structure turbulence strength, and the increased receiver aperture diameter and operating laser signal wavelength, this results in the increased signal to noise ratio, and the decreased laser intensity fluctuations, and bit error rates. As well as it is observed that the increased coding levels (positions or amplitudes), this leads to increase in bit rate, bandwidth efficiency, and signal to noise ratio, expect for NRZ-OOK, RZ-OOK which they are kept constant, and QAM which is dramatically decreased in bit rate, bandwidth efficiency. Moreover it is theoretically indicated that the increased minimum detectable received power with increasing receiver diameter and decreasing its responsitivity depend on its type.

REFERENCES

[1] N. S. Singh, G. Singh, "Performance Evaluation of Log-normal And Negative Exponential Channel Modeling Using Various Modulation Techniques in OFDM-FSO Communication," International Journal of Computers & Technology, Vol. 4 No. 2, pp. 639-648, 2013.

[2] V. W. S. Cha. 2006. "Free-space optical communications," Journal Lightwave Technology, Vol. 24, No. 12, pp. 4750-4762, 2012.

[3] S. Awan, L. C. Horwarth and M.S. Khan, "Characterization of Fog and Snow Attenuations for Free Space optical Propagation," Journal of communications, Vol. 04, No. 8, pp. 533-545, 2011.

[4] M. Saleem , E. Leitgeh , M.S. Khan and C. Capsoni, "A New method of Predicting Continental Fog Conditions," Radio Engineering Vol. 19, No. .3, pp. 460- 465, 2012.

[5] K. Kazaura, K. Wakamori, M. Matsumoto, T. Higashino, K. Tsukamoto, and S. Komaki, "RoFSO: A universal platform for convergence of fiber and free-space optical communication networks," IEEE Commun. Mag., Vol. 48, No. 2, pp. 130–137, 2011.

[6] D. Kedar and S. Arnon, "Urban optical wireless communication networks: The main challenges and possible solutions," IEEE Commun. Mag., Vol. 42, No. 5, pp. S2–S7, 2013.

[7] K. Tsukamoto, A. Hashimoto, Y. Aburakawa and M. Matsumoto, "The case for free space," IEEE Microw. Mag., Vol. 10, No. 5, pp. 84–92, 2012.

[8] K. Seong, M. Mohseni and J. M. Cioffi, "Optimal Resource Allocation for OFDMA Downlink Systems," IEEE ISIT Conference, Vol. 02, No. 2, pp. 347-355, 2011.

[9] S. Hranilovic and A. Mostafa, "In-Field Demonstration of OFDM-Over-FSO," IEEE Photonics Technology Letters, Vol. 24, No. 8, pp. 132-137, 2012.

[10] S. Rosetti and G. E. Corazza, "OFDM Channel Estimation Based on Impulse Response Decimation: Analysis and Novel Algorithms," IEEE Transactions On Communications, Vol. 6, No. 7, pp. 326-367, 2012.

[11] W. Gappmair and M. Flohberger, "Error Performance Of Coded FSO Links In Turbulent," Atmosphere Modeled By Gamma-Gamma Distributions, IEEE Transactions On Wireless Communications, Vol. 8, No. 5, pp. 129-235, 2009.

[12] A. Bekkali , C. B. Naila, K. Kazaura, K. Wakamori, and M. Matsumoto, "Transmission Analysis of OFDM-Based Wireless Services Over Turbulent Radio-on-FSO Links Modeled by Gamma–Gamma Distribution," IEEE Photonic Journal , Vol. 2, No. 3, pp. 510-520, 2010.

[13] W.O. Papoola and Z. Ghassemloo, "BPSK Subcarrier Intensity Modulated Free Space Optical Communications in Atmospheric Turbulence," Journal of Lightwave Technology, Vol. 27, No. 8, pp. 967-973 , 2009.

[14] L. C. Andrews, "Field Guide to Atmospheric Optics," The Society of Photo-Optical Instrumentation Engineers, Vol. 02, No. 1, pp. 59-66, 2013.

[15] Yi Xiang, Liu. Zengji, Yue Peng and Shang Tao, "BER performance analysis for M-ary PPM over gamma-gamma atmospheric turbulence channels," Proceeding of the 6th International Conference on Networking and Mobile Computing (WiCom), Chengdu, pp. 1-4, 2010.

[16] S. Hranilovic, Wireless Optical Communication Systems, Springer Science + Business Media, Boston, 2008.

[17] Zheng Zheng Juanjuan Yan and Anshi Xu Weiwei Hu, "Improved performance of M-ary PPM free-space optical communication systems in atmospheric turbulence due to forward error correction," Proceeding of the 10th International Conference on Communication Technology (ICCT), Guilin, pp.1- 4, 2006.

[18] Kamran Kiasaleh, "Performance of APD-based, PPM free-space optical communication systems in atmospheric turbulence," IEEE Transactions on Communications, vol. 53, pp.1455-1461, Sep. 2009.

Author's Profile

Dr. Ahmed Nabih Zaki Rashed was born in Menouf city, Menoufia State, Egypt country in 23 July, 1976. Received the B.Sc., M.Sc., and Ph.D. scientific degrees in the Electronics and Electrical Communications Engineering Department from Faculty of Electronic Engineering, Menoufia University in 1999, 2005, and 2010 respectively. Currently, his job carrier is a scientific lecturer in Electronics and Electrical Communications Engineering Department, Faculty of Electronic Engineering, Menoufia university, Menouf. Postal Menouf city code: 32951, EGYPT. His scientific master science thesis has focused on polymer fibers in optical access communication systems. Moreover his scientific Ph. D. thesis has focused on recent applications in linear or nonlinear passive or active in optical networks. His interesting research mainly focuses on transmission capacity, a data rate product and long transmission distances of passive and active optical communication networks, wireless communication, radio over fiber communication systems, and optical network security and management. He has published many high scientific research papers in high quality and technical international journals in the field of advanced communication systems, optoelectronic devices, and passive optical access communication networks. His areas of interest and experience in optical communication systems, advanced optical communication networks, wireless optical access networks, analog communication systems, optical filters and Sensors. As well as he is editorial board member in high academic scientific International research Journals. Moreover he is a reviewer member in high impact scientific research international journals in the field of electronics, electrical communication systems, optoelectronics, information technology and advanced optical communication systems and networks. His personal electronic mail ID (E-mail:ahmed_733@yahoo.com). His published paper under the title **"High reliability optical interconnections for short range applications in high performance optical communication systems"** in Optics and Laser Technology, Elsevier Publisher has achieved most popular download articles in 2013.

Dr. Hamdy A. Sharshar was born in Menouf city, Menoufia State, Egypt country in 24 July, 1956. Received the B.Sc., M.Sc., and Ph.D. scientific degrees in the Electronics and Electrical Communications Engineering Department from Faculty of Electronic Engineering, Menoufia University in 1979, 1987, and 1993 respectively. Currently, his job carrier is Asscoc. Prof. Dr. in Electronics and Electrical Communications Engineering Department, Faculty of Electronic Engineering, Menoufia university, Menouf 32951, Egypt. His scientific master science thesis has focused on **Electromagnetic scattering by plane and curved surfaces**. As well as his scientific Ph. D. thesis has focused on **Helical Antennas**. His interesting research mainly focuses on wireless communication, radio over fiber communication systems, and optical network security and management. His areas of interest and experience in wireless optical access networks, analog communication systems, optical filters and Sensors, network management systems and optical access computing systems.

